

# EPJ E

Soft Matter and  
Biological Physics

EPJ.org  
your physics journal

Eur. Phys. J. E (2011) **34**: 22

DOI: 10.1140/epje/i2011-11022-y

## **Influence of the electric field on the electron transport in photosynthetic reaction centers**

M. Pudlak and R. Pincak



Società  
Italiana  
di Fisica



Springer

# Influence of the electric field on the electron transport in photosynthetic reaction centers

M. Pudlak<sup>a</sup> and R. Pincak<sup>b</sup>

Institute of Experimental Physics, Slovak Academy of Sciences, Watsonova 47, 043 53 Kosice, Slovak Republic

Received 11 November 2010

Published online: 7 March 2011 – © EDP Sciences / Società Italiana di Fisica / Springer-Verlag 2011

**Abstract.** The effect of an electric field on the electron transfer in the bacterial reaction centers is investigated. The rate constants and quantum yields affected by the electric field for wild type (WT) and reaction center (RC) mutant of *Rhodobacter capsulatus* were computed. The dependence of the asymmetry of electron transfer in electric field on the temperature was evaluated. We found stable electron transfer for WT of the reaction center towards an electric field in comparison with the F(L121)D mutant of RC. We found quantum yields sensitive to the variation of the medium reorganization energy at low temperatures and strong electric fields. The quantum yields for unoriented RC samples were also calculated.

## 1 Introduction

The problem of bacterial photosynthesis attracts much interest since the reaction center (RC) of bacteria provides an interesting system for studying a high-efficiency electron transfer in an organized molecular complex. The photosynthetic reaction center [1] is a special pigment-protein complex, that functions as a photochemical trap. The reaction centers (RC) of purple bacteria are composed of three protein subunits called L, M and H [2,3]. All cofactors involved in the electron transfer (ET) are non-covalently bound to subunits L and M in two chains. Both chains of cofactors start at the bacteriochlorophyll dimer (P) which interacts with both subunits L and M. Then the cofactor chains are split and each individual one continues on the subunit L and symmetrically on the subunit M. Cofactors in the subunit L are accessory bacteriochlorophyll ( $B_L$ ), bacteriopheophytin ( $H_L$ ) and quinone ( $Q_L$ ). Identically, in the M subunit there are the accessory bacteriochlorophyll ( $B_M$ ), bacteriopheophytin ( $H_M$ ) and quinone ( $Q_M$ ). The arrangement of cofactors shows the local twofold symmetry. For more details on structural arrangement, see [4]. The cofactors serve as donor-acceptor pairs in the electron transfer. A remarkable aspect of the RC structures is the occurrence of two almost identical electron acceptor pathways arranged along the  $C_2$  axis relative to the primary charge-separating bacteriochlorophyll dimer P. In spite of the structural symmetry of the cofactors, the RC is functionally highly asymmetric. The pathway symmetry is broken by differences in amino acids around the cofactors. This asymmetry can lead to free energy, electronic coupling constants or molecular dynam-

ics differences between the L and M protein subunits. All these factors have a strong impact on the electron transfer in the reaction centers [5–7]. We focus in this paper on the influence of the electric field on the ET asymmetry in photosynthetic reaction centers of *Rhodobacter capsulatus* and their mutant F(L121)D. The effect of the electric field on the electron transfer in the L subunit and the spectra of the chromophores in the reaction centers was studied in earlier works [8–14]. In [13], the quantum yields of charge separation dependence on the electric fields at room temperature was measured using multilayer Langmuir-Blodgett films of RCs from *Rb. sphaeroides*. In their experiments, it was supposed that the RC is oriented and the electric fields are vectorially directed to hinder the charge separation. They found that the quantum yield of the  $P^+Q_L^-$  state decreases from a value of 0.96 at a zero field to about 0.75 for a field of 1.2 MV/cm.

The effect of an electric field on RCs from *Rb. sphaeroides* embedded in polyvinyl alcohol in a randomly oriented system was investigated in the work [10]. Upon application of a field of 0.7 MV/cm at 90 K, they observed a reduction of the quantum yield of  $P^+H_L^-$  by  $11 \pm 1.5\%$ .

The absence of an electric-field effect on the initial step was reported in [12]. Applying a field of nearly 1 MV/cm to the oriented RCs system there was found out a small effect on the quantum yields. A nearly 50:50 vectorial orientation of reaction centers parallel and antiparallel to the native reaction center orientation was assumed.

The effect of an applied electric field on the kinetics of the initial electron transfer reaction in *Rb. sphaeroides* reaction centers has been measured in an isotropic sample at 77 K [14]. Application of an electric field of 1 MV/cm at 77 K slightly reduces the formation of  $P^+H_L^-$ . No evidence was found for electron transfer down the M side of the reaction center.

<sup>a</sup> e-mail: pudlak@saske.sk

<sup>b</sup> e-mail: pincak@saske.sk

In the present paper, we describe the 6-site kinetic model affected by the electric field where all cofactors participating in ET on both branches L, M are taken into account. In [8, 15], the M branch cofactor has not been taken into account and the L side electron transfer was treated. More sites from which the system can decay into the ground state were assumed in [8]. The only possibility of the system decay in to the ground state from the primary donor ( $P^*$ ) is used in the present paper. The mechanism of primary charge separation was investigated and the backward electron transfer was neglected in [16]. The importance of backward reactions to elucidate the charge separation in bacterial photosynthesis has been shown in [8, 17]. To compute the quantum yields of the charge separation in the reaction center, the generalized master equations are used in the presented paper. It was shown in [17] that in the computation of quantum yields the integrals of the memory functions can be used. In the previous works, the Markovian approximation was explored and these integrals were used as rate constants to describe the electron transfer kinetics in the photosynthetic reaction centers.

Unidirectional electron transfer in wild-type RC is thought to be governed by differences between the free energies of charge separated states on the L and M branches and differences in electronic coupling factors between the cofactors on the two branches. To describe such a complex system as a reaction center, we need a lot of parameters. Still there is an ambiguity how to choose a correct set of parameters. The effect of the electric field on the quantum yields and the rate constants at different temperatures can help to get an accurate set of parameters which elucidate the electron transfer in the bacterial reaction centers. We want to show that there is some gap between theory and experiment which ought to be closed to get an appropriate description of the reaction centers.

## 2 Model of reaction center

The RC is a complex system. This system cannot be described as a closed system, because after some time, there ought to be a Boltzman distribution of electron localization on cofactors, and consequently, both branches had to be active. So we have to introduce a sink parameter into the model to describe the leak of electrons from RC. We start by considering an electron transfer system in which the electron has  $N$  accessible sites embedded in a medium. We denote by  $|j\rangle$  the state with electron localized at the  $j$ -th site and  $j = 1, 2, \dots, N$ . The  $j$  and  $k$  sites are coupled by  $V_{jk}$ . The interaction of the solvent with the system depends on the electronic states  $|j\rangle$  by  $H_j$ . The total model Hamiltonian for the system and medium is

$$H = H_0 + V, \quad (1)$$

where

$$H_0 = \sum_{j=1}^N |j\rangle [\varepsilon_j - i\Gamma_j + H_j - \mu_j F] \langle j|, \quad (2)$$

$$V = \sum_{j,k=1}^N V_{jk} |j\rangle \langle k|, \quad j \neq k, \quad (3)$$

where  $\varepsilon_j$  is the site energy and  $\mu_j$  is the dipole moment of the  $j$ -th molecule;  $F$  is the applied external electric field. The sink parameter  $\hbar/2\Gamma_j$  has the meaning of the lifetime of the electron at site  $j$  in the limit of the zero-coupling parameter. It can characterize the possibility of the electron escape from the system by another channel, for instance, a non-radiative internal conversion or recombination process. The Hamiltonian describing the reservoir consisting of harmonic oscillators is

$$H_j = \sum_{\alpha} \left\{ \frac{p_{\alpha}^2}{2m_{\alpha}} + \frac{1}{2} m_{\alpha} \omega_{\alpha}^2 (x_{\alpha} - d_{j\alpha})^2 \right\}. \quad (4)$$

Here,  $m_{\alpha}$  and  $\omega_{\alpha}$  are the frequency and the mass of the  $\alpha$ -th oscillator, and  $d_{j\alpha}$  is the equilibrium configuration of the  $\alpha$ -th oscillator when the system is in the electronic state  $|j\rangle$ . We describe ET in RC by the following kinetic model:

$$\begin{aligned} \partial_t P_1(t) = & -\frac{2\Gamma_1}{\hbar} P_1(t) - \int_0^t W_{12}(t-\tau) P_1(\tau) d\tau \\ & - \int_0^t W_{13}(t-\tau) P_1(\tau) d\tau \\ & + \int_0^t W_{21}(t-\tau) P_2(\tau) d\tau \\ & + \int_0^t W_{31}(t-\tau) P_3(\tau) d\tau, \end{aligned} \quad (5a)$$

$$\begin{aligned} \partial_t P_2(t) = & - \int_0^t W_{24}(t-\tau) P_2(\tau) d\tau \\ & - \int_0^t W_{21}(t-\tau) P_2(\tau) d\tau \\ & + \int_0^t W_{12}(t-\tau) P_1(\tau) d\tau, \end{aligned} \quad (5b)$$

$$\begin{aligned} \partial_t P_3(t) = & - \int_0^t W_{35}(t-\tau) P_3(\tau) d\tau \\ & - \int_0^t W_{31}(t-\tau) P_3(\tau) d\tau \\ & + \int_0^t W_{13}(t-\tau) P_1(\tau) d\tau \\ & + \int_0^t W_{53}(t-\tau) P_5(\tau) d\tau, \end{aligned} \quad (5c)$$

$$\begin{aligned} \partial_t P_5(t) = & - \int_0^t W_{53}(t-\tau) P_5(\tau) d\tau \\ & - \int_0^t W_{56}(t-\tau) P_5(\tau) d\tau \\ & + \int_0^t W_{35}(t-\tau) P_3(\tau) d\tau. \end{aligned} \quad (5d)$$

Here  $P_i(t)$  is the occupation probability of the site  $i$  and  $W_{ij}(t)$  is a memory function [17].

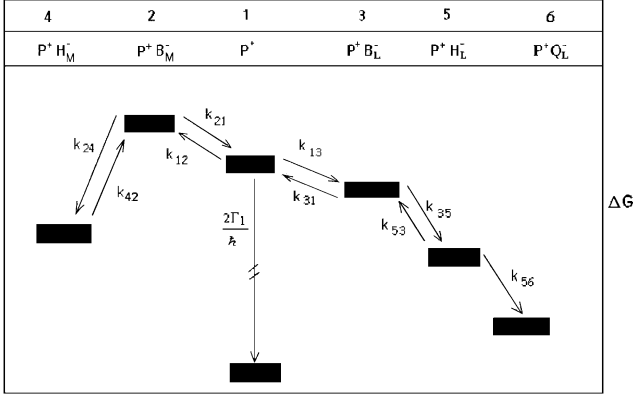


**Fig. 1.** Kinetic scheme for the primary electron transfer in bacterial photosynthetic reaction centers.

To describe the first steps of electron transfer processes in the reactions centers, we have used the 6-site model, see fig. 1. We designate the special pair P as site 1, sites 2 and 3 represent the molecules B<sub>M</sub> and B<sub>L</sub>, and sites 4 and 5 then represent the molecules H<sub>M</sub> and H<sub>L</sub>. Site 6 represents the quinone molecule Q<sub>L</sub>. We assume that this system is coupled to a bath (medium). Based on experimental observations of ET in RC, it is expected that bacteriochlorophyll plays a crucial role in ET. In this 6-site model we have assumed that ET in RC is sequential, where P<sup>+</sup>B<sup>-</sup> is a real chemical intermediate. The imaginary part of energy level 1 describes the probability of electron deactivation to the ground state.

### 3 Electronic escape through the branches

The quantum yields (QYs)  $\phi_L$ ,  $\phi_M$  of the electronic escape via the branches L and M, and the quantum yields  $\phi_G$  of the direct ground-state recombination can be characterized by the expressions

$$\phi_G = \frac{2\Gamma_1}{\hbar} \int_0^\infty P_1(t) dt = \frac{2\Gamma_1}{\hbar} P_1(s \rightarrow 0^+), \quad (6a)$$

$$\begin{aligned} \phi_M &= \int_0^\infty \int_0^t W_{24}(t-\tau) P_2(\tau) d\tau dt \\ &= k_{24}(s \rightarrow 0^+) P_2(s \rightarrow 0^+), \end{aligned} \quad (6b)$$

$$\begin{aligned} \phi_L &= \int_0^\infty \int_0^t W_{56}(t-\tau) P_5(\tau) d\tau dt \\ &= k_{56}(s \rightarrow 0^+) P_5(s \rightarrow 0^+), \end{aligned} \quad (6c)$$

where  $P_i(s)$ ,  $k_{ij}(s)$  are the Laplace transformations of  $P_i(t)$  and  $W_{ij}(t)$ . The quantum yields must fulfill the expression  $\phi_G + \phi_M + \phi_L = 1$ . We assume that the rate constant which characterizes ET can be described by both a low-frequency medium vibrational mode  $\omega_m$  and a high-frequency intramolecular vibrational mode  $\omega_c$ . We will work in the limit where the molecular modes are frozen,  $\hbar\omega_c \gg k_B T$ . In this regime the constant  $k_{ij}$  is in the

form [8, 18]

$$\begin{aligned} k_{ij} &= \int_0^\infty W_{ij}(t) dt = \frac{2\pi V_{ij}^2}{\hbar^2 \omega_m} \exp(-S_{cij} - S_m(2\bar{n}_m + 1)) \\ &\times \sum_{n=0}^\infty \frac{S_{cij}^n}{n!} \left( \frac{\bar{n}_m + 1}{\bar{n}_m} \right)^{p(n)/2} I_{|p(n)|} \left( 2S_m[\bar{n}_m(\bar{n}_m + 1)]^{1/2} \right). \end{aligned} \quad (7)$$

Here,  $p(n) = (G_{ij} - n\hbar\omega_c)/\hbar\omega_m$ ,  $G_{ij} = \epsilon_i - \epsilon_j - \Delta\mu_{ij}F_{\text{int}}$  and  $S_{cij} = \frac{1}{2\hbar} m_{cij}\omega_{cij}(d_{ci} - d_{cj})^2$  is the scaled reorganization constant of the high-frequency  $ij$ -th mode when the electron is transferred from the state  $|i\rangle$  to the state  $|j\rangle$ , and  $S_{mij} = \frac{1}{2\hbar} m_{mij}\omega_{mij}(d_{mi} - d_{mj})^2$  is the scaled reorganization constant of the low-frequency mode.  $I_p(z)$  is the modified Bessel function of order  $p$  and  $\bar{n}_m = [\exp(\frac{\hbar\omega_m}{k_B T}) - 1]^{-1}$ .  $\Delta\mu_{ij}$  is the difference in dipole moment vectors of the pertinent ion pair states. From the above expression we can see that the free energy of a radical pair with the dipole moment  $\mu$  in RC is perturbed by an amount  $-\Delta\mu_{ij}F_{\text{int}}$  in the presence of an applied external electric field  $F_{\text{ext}}$  [8, 19]. Because of the polarization of the surrounding medium  $F_{\text{int}} = fF_{\text{ext}}$ , where local field correction  $f$  is [20]

$$f = \frac{3\epsilon_{\text{PVA}}}{2\epsilon_{\text{PVA}} + \epsilon_{\text{RC}}} \frac{3\epsilon_{\text{RC}}}{2\epsilon_{\text{RC}} + \epsilon'}. \quad (8)$$

Here,  $\epsilon_{\text{PVA}}$ ,  $\epsilon_{\text{RC}}$  and  $\epsilon'$  denote the dielectric constants of poly (vinyl alcohol) (PVA) film, RC and cofactors, respectively. We assume that both the PVA and RC dielectric constants are equal but depend on temperatures. The dielectric constant of PVA has been measured to be about 4 at 80 K and 8 at 290 K [20, 21]. We assume that the dielectric constants of cofactors do not depend on temperature. We consider asymmetry of the dielectric constant of the cofactor on the M and L branches. We use  $\epsilon' = 1.6$  for M-side cofactors and  $\epsilon' = 4$  for L-side cofactors [22]. At  $T = 80$  K, if one chooses  $\epsilon' = 1.6$  and  $\epsilon_{\text{PVA}} = \epsilon_{\text{RC}} = 4$ , then  $f = 1.25$ . This value of  $f$  was used in computation for M-side electron transfer at  $T = 77$  and 9 K. For L-side electron transfer at these temperatures using  $\epsilon' = 4$  we get  $f = 1$ . At  $T = 290$  K, if one chooses  $\epsilon' = 1.6$  and  $\epsilon_{\text{PVA}} = \epsilon_{\text{RC}} = 8$ , then  $f = 1.36$ . This value of  $f$  was used in computation for M-side electron transfer at  $T = 295$  and 200 K. For L-side electron transfer at these temperatures using  $\epsilon' = 4$  we get  $f = 1.2$ . Computed local field corrections for both L and M branches of the reaction center are collected in table 1. We used the values in table 1 for all our computations of WT of RC and also for F(L121)D mutant of RC. It was assumed that at the initial time the electron was localized in the first molecule. The implementation of the theory requires information regarding the energetic parameters, medium reorganization energies, high- and low-frequency modes, and electronic coupling constants. Since electron transfer kinetics in *Rhodobacter Capsulatus* is similar to kinetics of *Rb. sphaeroides*, we adapt in this work the set of parameters that characterizes the observed L-side experimental kinetics of the wild-type *Rb. sphaeroides* reaction

**Table 1.** Computed local field correction  $f$  at different temperatures for M and L branch of the reaction center.

branch	$T$ K	$\varepsilon_{\text{PVA}}$	$\varepsilon_{\text{RC}}$	$\varepsilon'$	$f$
M	295	8	8	1.6	1.36
	200	8	8	1.6	1.36
	77	4	4	1.6	1.25
	9	4	4	1.6	1.25
L	295	8	8	4	1.2
	200	8	8	4	1.2
	77	4	4	4	1
	9	4	4	4	1

centers [8,15]: the high-frequency modes have the same value  $\hbar\omega_{cij} = 1500 \text{ cm}^{-1}$  besides  $\hbar\omega_{c56} = 1600 \text{ cm}^{-1}$ , the values  $V_{12} = V_{13} = 32 \text{ cm}^{-1}$ ,  $V_{24} = V_{35} = 59 \text{ cm}^{-1}$  and  $V_{56} = 4.8 \text{ cm}^{-1}$  for the electronic coupling constants, and  $S_{cij} = 0.5$  for the scaled reorganization constants for the high-frequency  $ij$  mode with only one distinguished value which is  $S_{c56} = 1$ , low-frequency mode  $\hbar\omega_{mij} = 80 \text{ cm}^{-1}$  with scaled reorganization constants  $S_{mij} = 10$ . The value  $\hbar\omega_{mij} = 80 \text{ cm}^{-1}$  for low-frequency medium mode was chosen in accordance with the results of work [7].

The value  $S_{mij} = 10$  of the scaled reorganization energy constant was used for each step of electron transfer to get the reorganization energy of the medium mode  $\lambda_m = \hbar\omega_m S_m = 800 \text{ cm}^{-1}$ . The exception is the electron transfer from the molecule of bacteriopheophytin (5) to the quinone molecule (6), where it was assumed that  $S_{m56} = 60$  to get the scaled reorganization energy  $4800 \text{ cm}^{-1}$  [8].

The energetic parameters for WT of RC at room temperature in the L branch are:  $\epsilon_1 = 0$ ,  $\epsilon_3 = -450 \text{ cm}^{-1}$ ,  $\epsilon_5 = -2000 \text{ cm}^{-1}$ ,  $\epsilon_6 = -7200 \text{ cm}^{-1}$ . The  $\text{P}^*$  internal conversion rate is  $\frac{2\Gamma_1}{\hbar} = (170 \text{ ps})^{-1}$  [8].

Much less is known about parameters characterizing the M side of the RC. It is thought that both  $\text{P}^+\text{H}_\text{M}$  and  $\text{P}^+\text{B}_\text{L}^-$  are at higher free energy than their L-side counterparts [23–27]. Calculation placed the free energy of  $\text{P}^+\text{H}_\text{M}$  at least  $1000 \text{ cm}^{-1}$  above  $\text{P}^+\text{H}_\text{L}^-$  [23,24] and  $\text{P}^+\text{B}_\text{M}$  above  $\text{P}^+\text{B}_\text{L}^-$  by  $1000\text{--}2800 \text{ cm}^{-1}$  [25–27]. For the present study the following parameters were selected for free energies to describe the electron transfer in the M branch of the wild type of the reaction center:  $\epsilon_2 = 800 \text{ cm}^{-1}$ ,  $\epsilon_4 = -1000 \text{ cm}^{-1}$ . In a series of *Rhodobacter capsulatus* RC mutants [28] the F(L121)D mutant shows 78% of the electron transfer to the L-side cofactors and 22% recombination to the ground state at room temperatures. The suggested model for the F(L121)D mutant assumed that  $\text{P}^+\text{H}_\text{L}^-$  has a higher free energy than in the wild type of RC, thus we had to increase the energy  $\epsilon_5$  from the value  $\epsilon_5 = -2000 \text{ cm}^{-1}$  to the value  $\epsilon_5 = -450 \text{ cm}^{-1}$ . To characterize the structural changes on the L branch in the F(L121)D mutant, we also slightly changed the free energy of the  $\text{P}^+\text{B}_\text{L}^-$  state and in the computation we used the value  $\epsilon_3 = -350 \text{ cm}^{-1}$ . Experimental observations in the F(L121)D mutant at low temperature (77 K) show 88%

quantum yield via the L side in comparison with 78% at room temperature. Due to the difficulty with detection of small ET to the M side in such mutants, there is, however, a probability of 5%–10% of ET to this side.

The results of our numerical computations for WT and mutant RC are collected in tables 2–5. In both branches only the sequential mechanism was assumed. We use for the calculations the following values of the dipole moments of individual cofactors:  $\mu(\text{P}^*) \simeq 0$ ,  $\mu(\text{P}^+\text{B}_{\text{L,M}}^-) = 51D$ ,  $\mu(\text{P}^+\text{H}_{\text{L,M}}^-) = 82D$  and  $\mu(\text{P}^+\text{Q}_\text{L}^-) = 134D$  [8]. Here we use approximations of the similarity of the difference in dipole moment vectors  $\Delta\mu_{ij}$  between cofactors on both branches [14,22]. We have assumed that the external electric field is parallel to the pseudo- $C_2$  axis of the RC. The field is defined as positive when directed from the non-heme Fe to the bacteriochlorophyll dimer P [8]. The comparison of theory with experimental data shows that there can be a decrease of medium reorganization energy with decrease of temperature [20,29]. To take into account this possibility, we compute also the quantum yields for reorganization energies  $\lambda_{mij} = 400 \text{ cm}^{-1}$  and  $\lambda_{m56} = 2400 \text{ cm}^{-1}$  at  $T = 77 \text{ K}$  and  $T = 9 \text{ K}$ . The results are depicted in fig. 2 and fig. 3.

## 4 Discussion

To explain the unidirectionality and also the experiments with mutant RCs, the six-site model was used. For this system the parameters, which describe electron transfer at the L branch, were employed. We used the free parameters symmetrically in both branches except the free energies of accessory bacteriochlorophylls and bacteriopheophytins. At the M branch we change only the free energy of accessory bacteriochlorophyll or bacteriopheophytin in comparison with the L branch. Variation of these free energies depends on the mutations.

In this paper, both the quantum yields and rate constants for WT and F(L121)D *Rhodobacter capsulatus* mutant RCs affected by the external electric field were computed. The results of our calculations are summarized in tables 2–5. We can see from tables 2 and 3 that the WT reaction center is stable towards an electric field (changes of  $\Phi_{\text{L(M)}}$  are very small). The noticeable decrease in  $\Phi_{\text{L(M)}}$  is found only at negative values of the electric field. We predict, similarly to the published study [14], that there is no electron transfer along the M branch of RC in the presence of an applied electric field. Table 4 describes how an increase of the positive field in the F(L121)D mutant decreases the parameter  $\Phi_\text{L}$ , mainly for  $T = 295 \text{ K}$ , representing the decline in probability of electron escape through the L branch. At the same time, this field enhances the probability of electron escape through the M branch, which is characterized by the value  $\Phi_\text{M}$ . With an increase of the negative value of the electric field (see table 5) yields  $\Phi_{\text{L(M)}}$  markedly decrease. The negative external electric field considerably increases the probability for deactivation of dimer  $\text{P}^*$  to the ground state.

The medium reorganization energy decreases with the decrease of temperature. This trend was documented



**Table 2.** The computed rate constant  $1/k_{ij}$  and quantum yields dependent on temperature and the positive values of the electric field for WT of reaction centers with asymmetry in the local field correction on different branches. The values of the electric field are shown in units of MV/cm. The energetic parameters in the calculations for WT of RC were chosen as:  $\epsilon_2 = 800 \text{ cm}^{-1}$ ,  $\epsilon_3 = -450 \text{ cm}^{-1}$ ,  $\epsilon_4 = -1000 \text{ cm}^{-1}$ ,  $\epsilon_5 = -2000 \text{ cm}^{-1}$  and  $\epsilon_6 = -7200 \text{ cm}^{-1}$ .

WT	$T$ K	$1/k_{12}$ ps	$1/k_{24}$ ps	$1/k_{13}$ ps	$1/k_{35}$ ps	$1/k_{56}$ ps	$\Phi_G$	$\Phi_M$	$\Phi_L$
$F = 0$	295	97	1.02	2.34	0.9	204	0.014	0.016	0.97
	200	513	1.2	2.1	1.1	187	0.012	0.002	0.986
	77	$3 \times 10^6$	2	1.9	3.3	166	0.01	0	0.99
	9	$3 \times 10^{55}$	4	2	11	166	0.01	0	0.99
$F = 0.5$	295	19	1.04	1.93	1.01	195	0.01	0.03	0.96
	200	46	1.01	1.6	1.2	179	0.01	0.005	0.985
	77	9030	0.9	1.1	2.8	165	0.01	0	0.99
	9	$7 \times 10^{31}$	0.9	0.9	9.3	178	0.01	0	0.99
$F = 1.5$	295	2.7	1.2	2.8	1.04	192	0.02	0.05	0.93
	200	2.6	1.03	3.3	0.95	180	0.02	0.01	0.97
	77	5.3	0.7	3.5	0.8	161	0.02	0	0.98
	9	15	0.6	5	0.7	152	0.03	0	0.97

**Table 3.** The computed rate constant  $1/k_{ij}$  and quantum yields dependent on temperature and the negative values of the electric field for WT of reaction centers with asymmetry in the local field correction on different branches. The values of the electric field are shown in units of MV/cm. For clarity we put the values smaller than  $10^{-4}$  equal to zero.

WT	$T$ K	$1/k_{12}$ ps	$1/k_{24}$ ps	$1/k_{13}$ ps	$1/k_{35}$ ps	$1/k_{56}$ ps	$\Phi_G$	$\Phi_M$	$\Phi_L$
$F = -0.5$	295	760	0.92	3.94	0.8	221	0.023	0.005	0.972
	200	11000	1.1	4.5	0.8	204	0.0260	0.0004	0.9736
	77	$4 \times 10^9$	3.5	8	1.65	170	0.05	0	0.95
	9	$9 \times 10^{79}$	14	38	2.9	152	0.18	0	0.82
$F = -1.5$	295	$2 \times 10^5$	0.63	31	0.6	290	0.1539	0.0002	0.8459
	200	$3 \times 10^7$	0.59	94	0.5	281	0.36	0	0.64
	77	$1 \times 10^{17}$	0.7	3030	0.5	218	0.95	0	0.05
	9	$2 \times 10^{130}$	0.8	$8 \times 10^{26}$	0.4	193	1	0	0

**Table 4.** The computed rate constant  $1/k_{ij}$  and quantum yields dependent on temperature and the positive values of the electric field for F(L121)D mutation of reaction centers with asymmetry in the local field correction on different branches. The values of the electric field are shown in units of MV/cm. The energetic parameters in the calculations for F(L121)D mutation of RC were chosen as:  $\epsilon_2 = 800 \text{ cm}^{-1}$ ,  $\epsilon_3 = -350 \text{ cm}^{-1}$ ,  $\epsilon_4 = -1000 \text{ cm}^{-1}$ ,  $\epsilon_5 = -450 \text{ cm}^{-1}$  and  $\epsilon_6 = -7200 \text{ cm}^{-1}$ .

F(L121)D	$T$ K	$1/k_{12}$ ps	$1/k_{24}$ ps	$1/k_{13}$ ps	$1/k_{35}$ ps	$1/k_{56}$ ps	$\Phi_G$	$\Phi_M$	$\Phi_L$
$F = 0$	295	97	1.02	2.65	1.2	206	0.12	0.13	0.75
	200	513	1.2	2.5	1.4	196	0.06	0.01	0.93
	77	$3 \times 10^6$	2	2.9	4	181	0.02	0	0.98
	9	$3 \times 10^{55}$	4	4.3	45	173	0.03	0	0.97
$F = 0.5$	295	19	1.04	2	0.83	221	0.10	0.25	0.65
	200	46	1.01	1.7	0.81	213	0.06	0.03	0.91
	77	9030	0.9	1.2	1.3	203	0.01	0	0.99
	9	$7 \times 10^{31}$	0.9	1	3	214	0.01	0	0.99
$F = 1.5$	295	2.7	1.2	2.6	0.6	272	0.11	0.32	0.57
	200	2.6	1.03	2.82	0.5	270	0.07	0.04	0.89
	77	5.3	0.7	2.3	0.4	258	0.01	0	0.99
	9	15	0.6	2.8	0.3	268	0.02	0	0.98

**Table 5.** The computed rate constant  $1/k_{ij}$  and quantum yields dependent on temperature for F(L121)D mutated reaction center. The values of the electric field are shown in units of MV/cm. For clarity we put the values smaller than  $10^{-4}$  equal to zero.

F(L121)D	$T$ K	$1/k_{12}$ ps	$1/k_{24}$ ps	$1/k_{13}$ ps	$1/k_{35}$ ps	$1/k_{56}$ ps	$\Phi_G$	$\Phi_M$	$\Phi_L$
$F = -0.5$	295	760	0.92	4.9	1.97	196	0.13	0.03	0.84
	200	10687	1.136	2	2.9	184	0.076	0.001	0.923
	77	$4 \times 10^9$	3.5	18	19	167	0.09	0	0.91
	9	$9 \times 10^{79}$	14	281	$5 \times 10^6$	149	0.62	0	0.38
$F = -1.5$	295	162581	0.63	47	7.7	192	0.2929	0.0003	0.7068
	200	$2 \times 10^7$	0.59	177	22	178	0.52	0	0.48
	77	$1 \times 10^{17}$	0.7	13424	1270	162	0.99	0	0.01
	9	$2 \times 10^{130}$	0.8	$4 \times 10^{33}$	$1 \times 10^{28}$	161	1	0	0

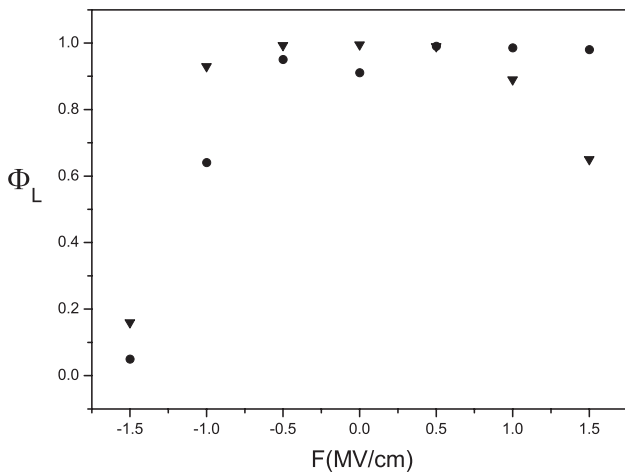


**Fig. 2.** Comparison of the quantum yield through the branch L *versus* the electric field in the case of WT reaction centers for different medium reorganization energies at  $T = 77$  K. In the computations the reorganization energies  $\lambda_{mij} = 800 \text{ cm}^{-1}$ ,  $\lambda_{m56} = 4800 \text{ cm}^{-1}$  (●) and  $\lambda_{mij} = 400 \text{ cm}^{-1}$ ,  $\lambda_{m56} = 2400 \text{ cm}^{-1}$  (▼) were used.

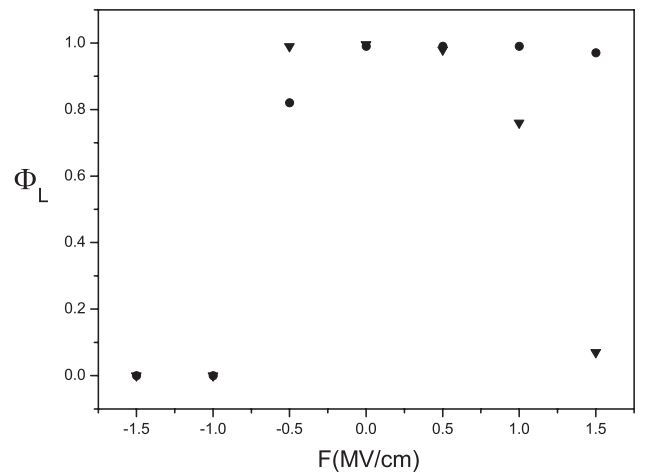


**Fig. 3.** Comparison of the quantum yield through the branch L *versus* the electric field in the case of WT reaction centers for different medium reorganization energies at  $T = 9$  K. In the computations the reorganization energies  $\lambda_{mij} = 800 \text{ cm}^{-1}$ ,  $\lambda_{m56} = 4800 \text{ cm}^{-1}$  (●) and  $\lambda_{mij} = 400 \text{ cm}^{-1}$ ,  $\lambda_{m56} = 2400 \text{ cm}^{-1}$  (▼) were used.

in [20]. The dependence of the quantum yield through the branch L on the applied field is depicted in figs. 2 and 3. It can be seen that at low temperature two possible values of medium reorganization energies gives very different quantum yields. So we have a possibility to determine the reorganization energy of medium at low temperature. In a similar way we can control the free energies of the cofactor.

The dielectric constant asymmetry between the M and L branches was taken into account in the computation. The temperature dependence of the local field was included in the computations. So the asymmetry of the local field on both branches was imposed into the model, eq. (8), table 1.

We can see from table 4 that the quantum yield via the L-side for the F(L121)D mutant at low temperature is not in accordance with experimental observations. The computed value in table 4 is 98% in contrast with the observed value at temperature 77 K which is 88% [28]. To obtain the observed result, we have to modify parameters

in our model. More precisely, we must assume that asymmetry in the electronic coupling exists. We used, similarly as in [29], the following asymmetry in electronic coupling:  $V_{12} = 10 \text{ cm}^{-1}$  and  $V_{13} = 15 \text{ cm}^{-1}$ . We get the following  $\Phi_L$ : 0.75 at 295 K, 0.89 at 200 K, 0.92 at 77 K and 0.9 at 9 K. Only with this asymmetry in the electronic coupling can we fit the experimental results at 77 K. We have to stress that it is the only possibility which can describe the quantum yields also at 77 K. This modification of hopping terms changes also the dynamical characteristic of the system as the electron transfer rates. This also gives the opportunity to check the theoretical prediction by experiments. There is a lack of information about quantum yields at low temperature (9 K) to verify the theoretical model.

The correction above confirmed that RC are very complex systems where all parameters influenced the final asymmetry in the electron transfer. To describe the electron transfer kinetics in the reaction centers, several free

**Table 6.** The computed quantum yields for unoriented RC samples where the parameters were chosen as  $\alpha = \beta = 0.5$ .

$F = \pm 1.5$	$T$ (K)	$\Phi_G$	$\Phi_M$	$\Phi_L$
WT	295	0.08	0.03	0.89
	200	0.19	0.01	0.8
F(121L)D	295	0.2	0.16	0.64
	200	0.29	0.02	0.69

parameters were used. These parameters cannot yet be determined by experiment directly. Our model, where the temperature dependence of quantum yields with and without electric fields is computed, can help to find the value of the parameters that characterize the reaction centers.

Up to now we used in our computations only oriented RC samples [12]. Now we would like to extend our discussion also to unoriented RC samples [13]. In order to extend our model to an unoriented RC samples, we denote quantum yields affected by the positive electric field as  $\Phi_{L(M,G)}^\uparrow$  and similarly for the negative electric field  $\Phi_{L(M,G)}^\downarrow$ . It follows that full quantum yields for unoriented RC samples will have the form

$$\Phi_{L(M,G)} = \alpha \Phi_{L(M,G)}^\uparrow + \beta \Phi_{L(M,G)}^\downarrow, \quad (9)$$

where  $\alpha$  and  $\beta$  are the parameters describing the probabilities that RC are oriented in the positive and negative direction. In eq. (9) the condition  $\alpha + \beta = 1$  must be fulfilled. It means that  $\alpha = P_1/(P_1 + P_2)$  and  $\beta = P_2/(P_1 + P_2)$ , where  $P_1$  and  $P_2$  are the populations of RC in the Langmuir-Blodgett film in the positive and negative direction. Now we demonstrate the change of quantum yields in the case of the partially oriented film in comparison to the fully oriented film. The quantum yields for WT, and F(121L)D mutant of RC in the case of positive(negative) electric field  $F = \pm 1.5$  MV/cm were computed at room temperature. The results are shown in table 6. The experimental data depend on the parameters  $\alpha$ ,  $\beta$ . The ideal situation will be in the case when these parameters can be revealed in experiment. Knowing the value of the parameters  $\alpha$ ,  $\beta$ , we will be able to find the value of the quantum yields which could be compared with experimental data also for partially oriented RC samples.

In eq. (9) we neglected the term which describes the population of RCs that are neither aligned nor antialigned with the applied field. We think that if the sample contains also such population of RCs, the presented theory with electric fields cannot be used to elucidate the experimental data.

Now we used the approach described in the presented paper to discuss some experimental data where the effect of the electric field on the reaction centers from *Rb. sphaeroides* has been reported. We predict  $\Phi_L = 0.97$  for zero electric field at 295 K for the WT reaction centers. Applying the electric field  $F = -1.5$  MV/cm we get  $\Phi_L = 0.85$  (tables 2, 3). If we compare this prediction with experimental data [13], we see that the prediction and data are not in consistency. We predict not enough

decrease of  $\Phi_L$  with the electric field increase. The reason could be that we do not take into account the dependence of the parameter  $\Gamma_1$  and the reorganization energies on the applying electric field. There also could exist other states from which the electron can recombine directly into the ground state in addition to the  $P^*$  state. Such possibilities were used in the kinetic model of electron transfer in work [8] to elucidate the electric-field effect on quantum yields of charge separation.

The presented model predicts the following quantum yields for WT at 90 K:  $\Phi_G = 0.015$ ,  $\Phi_M = 0$ ,  $\Phi_L = 0.985$  for the applied electric field  $F = 1$  MV/cm and  $\Phi_G = 0.25$ ,  $\Phi_M = 0$ ,  $\Phi_L = 0.75$  for the applied electric field  $F = -1$  MV/cm. If we assume that we have a sample with  $\alpha = \beta = 1/2$ , we predict an average  $\Phi_L = 0.867$ . It means that we get a reduction of  $\Phi_L$  by 10% similarly to the experimental data [10]. There is a possibility that the main contribution to  $\Phi_L$  comes from the population of reaction centers aligned and antialigned to the applied electric field.

For comparison with the experimental results, the quantum yields for WT at 295 K have been computed:  $\Phi_G = 0.02$ ,  $\Phi_M = 0.04$ ,  $\Phi_L = 0.94$  for the applied electric field  $F = 1$  MV/cm and  $\Phi_G = 0.089$ ,  $\Phi_M = 0.001$ ,  $\Phi_L = 0.91$  for the applied electric field  $F = -1$  MV/cm. If we assume that we have a sample with  $\alpha = \beta = 1/2$ , we get the average  $\Phi_L = 0.925$ . So we predict a small effect of the electric field on the quantum yields similarly to the experimental results of [12]. We predict no electron transfer down the M side of the wild-type reaction centers due to the applied electric field, in accordance with the results of [14].

## 5 Conclusions

Valuable information about the system can be derived from the temperature dependence of the quantum yields. Typically, these measurements are performed at room temperature and 77 K. However, for comparison of the theoretical predictions with experiments, the data at more than two temperatures are required. Only a few experiments on the quantum yields extend measurements also to the low temperature (for instance 7 K). Under these experimentally restricted circumstances data can be fitted with several different sets of input parameters. If the theoretical predictions and experimental data are in accordance at two different temperatures, then obviously the set of input parameters are fixed and other data can confirm or disprove the theoretical model. This is the case of the F(L121)D mutant where QYs at 9 K can overturn the model.

With an applied electric field the free energy of the cofactors on both branches can be increased or decreased depending on the field orientation. Electron transfer is very sensitive to the relative free energy differences of charge separate state. The applied electric fields change these mutual differences and the result is different kinetics between cofactors. Probabilities to escape via the L and M branches are also modified. If the main reason for the asymmetry of



the electron transfer is the asymmetry of the free energy of cofactors on two branches, then quantum yields, or the probabilities of electron transfer in the L and M branches, must be dependent on the applied field. This dependence arises from the influence of the field on the energy of cofactors. In case the asymmetry of the electronic coupling constants is responsible for the asymmetry of electron flow, the application of the field cannot change these probabilities. Our predictions are not in contrast with the published experimental data. Partial reduction of the quantum yields in the L subunit of RC due to the external electric field was observed in [30]. We obtained the results that are also in agreement with experimental data for the WT reaction centers. These data predict a weak influence of the positive electric field on the quantum yield. In the case of the negative electric field, the system decays into the ground state and there is no transfer of electron through the M branch. Our model, in contrast to the previous models where the option of electron escape through the M branch is not available, can explain these observations. We believe that our model improves the determination of free energies in the mutants and thus it contributes to better understanding of electron transfer in reaction centers. To hold the input parameters, we have to compare the prediction of a theoretical model with experimental data. Several experimental techniques are needed to get realistic values of these parameters. One of them can be the electric-field influence on the rate constants and quantum yields. Moreover, the electron transfer kinetics and its dependence on temperature can be computed. This brings additional information about the RC system. Thus, there is a number of points or areas where the theory and experiment can be compared and input parameters can be estimated.

The applied electric field is an additional controllable parameter in the ET system which can help to fix the set of input parameters. Our model with a unique set of parameters describes the behavior of quantum yields in the whole temperature range. Yet this prediction has to be verified by the collection of data for both mutants and wild-type reaction centers.

The regulation of the electron transport by the external electric field in mutants of RC or artificial reaction centers [31–34] opens a possible direction of several practical applications, *e.g.*, in microelectronics or energy conversion and storage.

The work was supported by the Slovak Academy of Sciences in the framework of CEX NANOFLUID, and by the Science and Technology Assistance Agency under Contract No. APVV 0509-07 and by VEGA Grant No. 2/0069/10.

## References

1. L.N.M. Duysens, *Biochim. Biophys. Acta* **19**, 188 (1956).
2. H. Michel, K.A. Weyer, H. Gruenberg, F. Lottspeich, *EMBO J.* **4**, 1667 (1985).
3. K.A. Weyer, F. Lottspeich, H. Gruenberg, H. Michel, *EMBO J.* **6**, 2197 (1987).
4. J. Deisenhofer, H. Michel, *EMBO J.* **8**, 2149 (1989).
5. R. Pincak, M. Pudlak, *Phys. Rev. E* **64**, 031906 (2001).
6. M. Pudlak, R. Pincak, *Chem. Phys. Lett.* **342**, 587 (2001).
7. M. Pudlak, R. Pincak, *Phys. Rev. E* **68**, 061901 (2003).
8. S. Tanaka, R.A. Marcus, *J. Phys. Chem. B* **101**, 5031 (1997).
9. A. Gopher, Y. Blatt *et al.*, *Biophys. J.* **48**, 311 (1985).
10. A. Ogrodnik, T. Langenbacher *et al.*, *Chem. Phys. Lett.* **198**, 653 (1992).
11. H. Zhou, S.G. Boxer, *J. Phys. Chem. B* **102**, 9139 (1998).
12. C.C. Moser *et al.*, *Chem. Phys.* **197**, 343 (1995).
13. Z.D. Popovic *et al.*, *Biochim. Biophys. Acta* **851**, 38 (1986).
14. D.J. Lockhart, Ch. Kirmaier *et al.*, *J. Phys. Chem.* **94**, 6987 (1990).
15. M. Bixon, J. Jortner, M.E. Michel-Beyerle, *Chem. Phys.* **197**, 389 (1995).
16. M. Bixon, J. Jortner, M.E. Michel-Beyerle, *Biochim. Biophys. Acta* **1056**, 301 (1991).
17. M. Pudlak, *J. Chem. Phys.* **118**, 1876 (2003).
18. J. Jortner, *J. Chem. Phys.* **64**, 4860 (1976).
19. S. Franzen, R.J. Stanley, *Chem. Phys.* **276**, 115 (2002).
20. S. Franzen, S.G. Boxer, *J. Phys. Chem.* **97**, 6304 (1993).
21. M. Losche, G. Feher, M.Y. Okamura, *Proc. Natl. Acad. Sci. U.S.A.* **84**, 7537 (1987).
22. M.A. Steffen, K. Lao, S.G. Boxer, *Science* **264**, 810 (1994).
23. R.C. Alden, W.W. Parson, Z.T. Chu, A. Warshel, *J. Phys. Chem.* **100**, 16761 (1996).
24. M.R. Gunner, A. Nicholls, B. Honing, *J. Phys. Chem.* **100**, 4277 (1996).
25. M.A. Thompson, M.C. Zerner, J. Fajer, *J. Am. Chem. Soc.* **113**, 8210 (1991).
26. M. Marchi, J.N. Gehlen, D. Chandler, M. Newton, *J. Am. Chem. Soc.* **115**, 4178 (1993).
27. M.R.A. Blomberg, P.E.M. Siegbahn, G.T. Babcock, *J. Am. Chem. Soc.* **120**, 8812 (1998).
28. B.A. Heller, D. Holten, C. Kirmaier, *Biochemistry* **35**, 15418 (1996).
29. M. Pudlak, R. Pincak, *J. Biol. Phys.* **36**, 273 (2010).
30. K. Lao, S. Franzen *et al.*, *Chem. Phys.* **197**, 259 (1995).
31. J.I. Chuang *et al.*, *J. Phys. Chem. B* **112**, 5487 (2008).
32. J.I. Chuang *et al.*, *Biochemistry* **45**, 3846 (2006).
33. H. Imahori *et al.*, *J. Am. Chem. Soc.* **123**, 6617 (2001).
34. G. Kodis *et al.*, *J. Phys. Org. Chem.* **17**, 724 (2004).